

Plaquette resonating valence bond state in a frustrated honeycomb antiferromagnet

R. Ganesh,^{1,*} Satoshi Nishimoto,¹ and Jeroen van den Brink^{1,2}

¹*Institute for Theoretical Solid State Physics, IFW Dresden, PF 270116, 01171 Dresden, Germany*

²*Department of Physics, Technical University Dresden, D-1062 Dresden, Germany*

(Received 26 September 2012; revised manuscript received 21 January 2013; published 13 February 2013)

We study the proposed plaquette resonating valence bond (pRVB) state in the honeycomb lattice J_1 - J_2 model with frustration arising from next-nearest-neighbor interactions. Starting with the limit of decoupled hexagons, we develop a plaquette operator approach to describe the pRVB state and its low-energy excitations. Our calculation clarifies that the putative pRVB state necessarily has f -wave symmetry: the plaquette wave function is an antisymmetric combination of the Kekulé structures. We estimate the plaquette ordering amplitude, ground-state energy, and spin gap as a function of J_2/J_1 . The pRVB state is most stable around $J_2/J_1 \sim 0.25$. We identify the wave vectors of the lowest triplet excitations, which can be verified using exact diagonalization or density-matrix renormalization group (DMRG) studies. When J_2 is reduced, we can have either a deconfined quantum phase transition (QPT) or a first-order transition into a Néel state. When J_2 is increased, we surmise that the system will undergo a first-order phase transition into a state which breaks lattice rotational symmetry.

DOI: [10.1103/PhysRevB.87.054413](https://doi.org/10.1103/PhysRevB.87.054413)

PACS number(s): 75.10.Jm

I. INTRODUCTION

Magnetic systems with frustrating interactions serve as an excellent route to generating novel quantum states with various degrees of entanglement. They often give rise to many-body ground states in which many constituents become entangled, from which new collective degrees of freedom emerge. Examples include valence bond solid (VBS) phases,¹ decoupled chains,² and spin liquids. At each level of entanglement, a new effective theory is needed to describe the low-energy properties of the system. In this light, we study a plaquette-ordered phase proposed as a ground state for the honeycomb lattice spin-1/2 J_1 - J_2 model, with frustration arising from next-nearest-neighbor couplings. This plaquette resonating valence bond (pRVB) phase comprises entangled hexagons, arranged in a $\sqrt{3} \times \sqrt{3}$ pattern.

Recently, the J_1 - J_2 model on the honeycomb lattice has generated tremendous interest as an effective model for the intermediate- U physics of the Hubbard model on the honeycomb lattice.³ It may also be relevant to the material $\text{Bi}_3\text{Mn}_4\text{O}_{12}(\text{NO}_3)$ which shows no long-range order down to the lowest temperatures.⁴⁻⁶ Being the simplest model of frustration on the honeycomb lattice, the J_1 - J_2 model has been extensively studied. In the semiclassical limit of large S , this model is very well understood: for small J_2 , the ground state has Néel order. At a critical value $J_2 = 1/6$ (we set $J_1 = 1$), there is a Lifshitz transition into a spiral state with extensive ground-state degeneracy. Order-by-disorder effects mediated by quantum/thermal fluctuations select three spiral states which are related by lattice rotations. The ground state thus breaks lattice rotational symmetry. By contrast, the extreme quantum limit of $S = 1/2$ is not well understood. In spite of many recent studies, the phase diagram has not yet been conclusively established. In particular, many studies point to an interesting intermediate phase for $0.2 \lesssim J_2 \lesssim 0.4$ which interpolates between Néel order and a state which breaks lattice rotational symmetry.

While all studies in the literature agree upon the existence of an intermediate phase, its precise nature has not been

established. Some proposals indicate that the intermediate state may be a Z_2 spin liquid.⁷⁻⁹ Others give support to a pRVB state which breaks translational symmetry.¹⁰⁻¹² A functional renormalization group study shows weak tendency to pRVB order,¹³ while a recent variational calculation does not find plaquette order.¹⁴ In the closely related J_1 - J_2 - J_3 model, coupled cluster calculations support pRVB order.¹⁵ In the light of such conflicting studies, we study the proposed pRVB state and suggest more precise tests to confirm its existence. It is worthwhile to devise such tests as most of the evidence for a pRVB ground state comes from calculations restricted to small system sizes. In addition, our study sheds light on the properties of this putative state, its low-energy excitations, and the nature of phase transitions into and out of this phase.

In this paper, we build an effective theory for the candidate pRVB state using a *plaquette-operator* approach. We estimate its ground-state energy and spin gap and determine the nature of low-energy excitations. Our goals are threefold: (i) to understand the nature of the pRVB state, (ii) to clarify the nature of phase transitions into and out of this state, and (iii) to suggest tests which can be carried out using numerical techniques such as the density-matrix renormalization group (DMRG). Such tests might conclusively reveal whether the pRVB state indeed arises in the J_1 - J_2 model.

This paper is organized as follows. In Sec. II, we begin with the $S = 1/2$ J_1 - J_2 model on a single hexagon. We classify all its eigenstates as a function of J_2/J_1 . Section III introduces the plaquette operator representation and lays out the formalism sequentially, by first considering two coupled hexagons and then tiling hexagons to form a honeycomb lattice. We argue that the pRVB state has f -wave character, rather than s -wave. We arrive at a simplified effective Hamiltonian that only involves triplet excitations. Section IV gives the results of the pRVB mean-field theory with spin gap, ground-state energy, and pRVB amplitude. Finally, Sec. V discusses the nature of phase transitions into and out of this phase and implications for the J_1 - J_2 model.

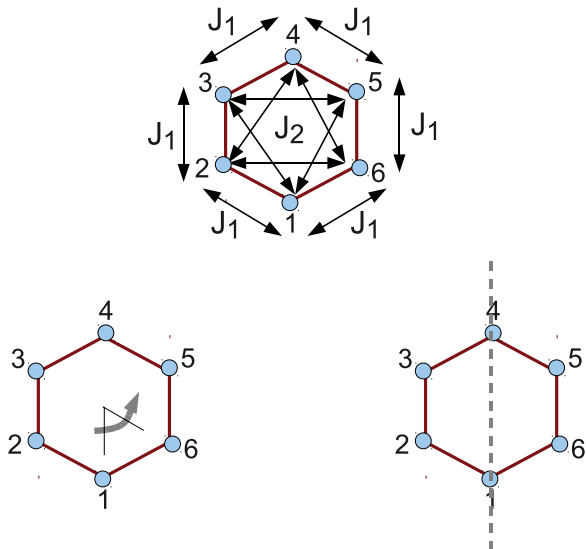


FIG. 1. (Color online) Top: Exchange couplings in the single-hexagon Hamiltonian. The following operations commute with the Hamiltonian: (bottom left) rotation by 60° , and (bottom right) inversion about an axis passing through opposite sites.

II. THE SINGLE HEXAGON PROBLEM

On a single hexagon, the spin-1/2 J_1 - J_2 model is easily diagonalized, with a Hilbert space of 64 ($=2^6$) states. The Hamiltonian is given by (we set $J_1 = 1$)

$$H_{\text{single-hex}} = \sum_{\langle ij \rangle} \mathbf{S}_i \cdot \mathbf{S}_j + J_2 \sum_{\langle\langle ij \rangle\rangle} \mathbf{S}_i \cdot \mathbf{S}_j. \quad (1)$$

We take the exchange couplings J_1 and J_2 to be positive. The J_1 and J_2 bonds are shown in Fig. 1.

As the Hamiltonian is invariant under global spin rotations, its eigenstates have well defined magnetic quantum numbers. Diagonalizing the Hamiltonian numerically, we obtain the spectrum consisting of 5 singlets ($S_{\text{tot}} = 0$), 27 triplets ($S_{\text{tot}} = 1$), 25 quintets ($S_{\text{tot}} = 2$), and 7 heptets ($S_{\text{tot}} = 3$). In the next section, we will argue that only one singlet and the 27 triplet states are relevant for understanding the pRVB phase.

The Hamiltonian is invariant under two spatial operations: (i) rotation by 60° , and (ii) mirror inversion about a line (see Fig. 1). As the two operations do not commute with each other, the eigenstates of the Hamiltonian cannot always be chosen to be simultaneously the eigenstates of both. For later convenience, we choose the eigenstates to be simultaneously eigenstates of rotation. Defining \hat{R} to be the rotation operator, we note that \hat{R}^6 is the identity operation. Therefore, the eigenvalues of \hat{R} are the sixth roots of unity.

We denote the states obtained by diagonalization as $|u\rangle$, with $u = 1, \dots, 64$ with the energy eigenvalues ϵ_u . Each state is assigned three quantum numbers (l_u, m_u, r_u) , where l_u and m_u are the usual magnetic quantum numbers, and r_u is the eigenvalue under rotation. For example, $(l_u, m_u, r_u) = (1, 0, -1)$ indicates that the state $|u\rangle$ is a triplet with $S_z = 0$ and it changes sign under rotation by 60° . Note that these three quantum numbers do not uniquely identify a state.

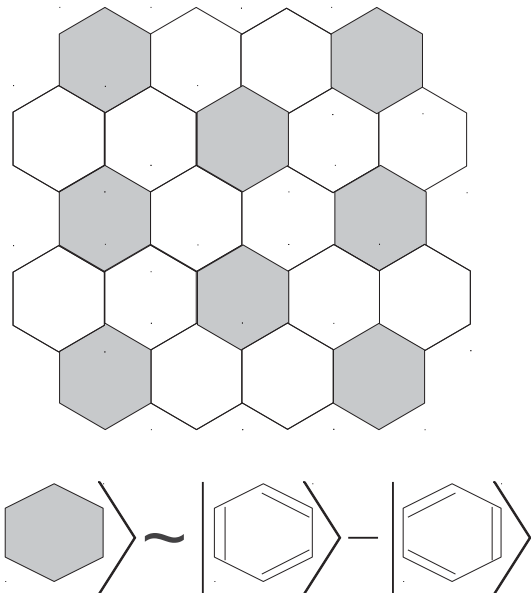


FIG. 2. The proposed pRVB state on the honeycomb lattice. The shaded hexagons are in an antisymmetric combination of the two singlet covers

As J_2 is varied, some of the the low energy states of the single hexagon problem are

- (i) “+” singlet: this state is the *symmetric* combination of the two Kekulé structures proposed for benzene. With quantum numbers $(0, 0, 1)$, it is invariant under rotation by 60° .
- (ii) “-” singlet: this is the ground state for $J_2 < 0.5$. It is predominantly ($\sim 98.5\%$; the precise fraction depends weakly on J_2) an *antisymmetric* combination of the Kekulé structures (see Fig. 2). With quantum numbers $(0, 0, -1)$, it is even under inversion and odd under rotation.

- (iii) t_1 triplets: these are the triplet states with the quantum numbers $(1, m, 1)$, with $m = -1, 0, 1$. They are invariant under rotation.

Figure 3 shows the low-energy spectrum of the single-hexagon problem as a function of J_2 . We only indicate the ground state and the first two excited states. The “-” singlet is the ground state for $J_2 < 0.5$. There is a level crossing at $J_2 = 0.5$ beyond which the “+” singlet becomes the ground state.

On the full honeycomb lattice, previous studies have suggested a plaquette-ordered ground state for $0.2 \lesssim J_2 \lesssim 0.4$.^{10–12} In this parameter regime, the ground state of the *single* hexagon problem is the “-” singlet. We argue that the

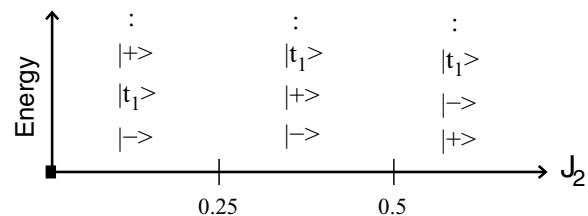


FIG. 3. Energy spectrum of the single hexagon problem; for brevity, we only show the lowest three states. The ground state is the “-” singlet for $J_2 < 0.5$. For $J_2 > 0.5$, the “+” singlet becomes the ground state. For $J_2 < 0.25$, the first excited states are the t_1 triplets. For $J_2 > 0.25$, the t_1 go higher in energy.

suggested plaquette-ordered state is composed of a $\sqrt{3} \times \sqrt{3}$ ordering of hexagons in the “-” state as shown in Fig. 2. The choice of the “-” state corresponds to f -wave pRVB order: the plaquette wave function changes sign upon rotation by 60° . In the next section, we describe the plaquette-operator method which provides a consistent scheme to include quantum fluctuations around this state.

III. PLAQUETTE OPERATOR THEORY

We obtain an effective theory of the pRVB state in analogy with the bond operator formalism of Sachdev and Bhatt.¹⁶ Developed in the context of dimer states in spin-1/2 systems, the bond operator method starts from the limit of isolated bonds; the ground state is then composed of disconnected dimers (singlets). A bosonic representation is introduced for the states of each bond in the singlet-triplet basis, with a constraint of unit boson occupancy to preserve the Hilbert space. The dimer state can now be elegantly described as a Bose condensate of singlet bosons. Moving away from the limit of isolated bonds, interbond coupling can be naturally interpreted as four-particle interactions between bosons. Assuming that dimer order is strong, one arrives at a mean-field prescription to treat the interaction terms which gives rise to a quadratic theory of “triplons”. Corrections beyond mean-field theory, viz., interactions between triplons, can be ignored as the triplons are present in dilute concentrations. This theory has been very successful in obtaining the spectrum of triplon excitations above the dimer state. The dimer-Néel phase transition is easily understood as the Bose-condensation of triplons with the bond-operator mean-field theory providing excellent quantitative estimates for the transition point (e.g., see Refs. 17 and 18).

This approach has been adapted to study plaquette order, albeit in a simple system with four-site plaquettes.^{19,20} Here, we develop a plaquette operator approach to describe six-site plaquette order in the honeycomb pRVB state.

Having obtained all eigenstates of the single hexagon problem in the previous section, we now introduce a bosonic representation for these states. We associate a boson with each of the 64 states in the Hilbert space. We call these “plaquette bosons”. To preserve the Hilbert space, we impose a constraint of unit boson occupancy. On a single hexagon, we may write

$$|u\rangle = b_u^\dagger |0\rangle. \quad (2)$$

Here, the operator b_u^\dagger creates a u boson when it acts upon the vacuum. The vacuum itself is an unphysical state, as it does not respect the unit occupancy constraint. Operators can also be translated into the new representation, e.g., $|v\rangle\langle u| \equiv b_v^\dagger b_u$.

Having solved the single hexagon problem exactly, we tile hexagons to form a two-dimensional honeycomb lattice, as shown in Fig. 2. The shaded hexagons serve as sites upon which plaquette bosons reside. As a starting point, we consider the limit of isolated plaquettes. Turning off all interplaquette couplings, we obtain a quadratic theory of bosons given by

$$H_{\text{intraplaq.}} = \sum_i \sum_u \epsilon_u b_{i,u}^\dagger b_{i,u}, \quad (3)$$

where the index i sums over all shaded plaquettes in Fig. 2; note that the shaded hexagons form a triangular lattice. The index

u sums over the 64 eigenstates of the single hexagon problem. The operator $b_{i,u}^\dagger$ creates a u boson at the site (plaquette) i .

The pRVB state can now be identified as a Bose condensate of the “-” bosons; i.e., we may set

$$b_{i,-} \equiv b_{i,-}^\dagger \equiv \bar{p}, \quad (4)$$

where \bar{p} is the Bose-condensation amplitude. Physically, the quantity \bar{p}^2 gives the probability of finding a shaded plaquette in the “-” state. We take \bar{p} to be real as its phase is not relevant in the present context. In the isolated plaquette limit, \bar{p}^2 is unity as every hexagon is entirely in the “-” state.

To preserve the Hilbert space, the total occupancy of bosons per plaquette should be unity. In the spirit of mean-field theory, we enforce this constraint on average using a chemical potential μ :

$$H \rightarrow H - \mu \left[N \bar{p}^2 + \sum_{i,u=2,\dots,64} b_{i,u}^\dagger b_{i,u} - N \right], \quad (5)$$

where N is the total number of shaded plaquettes in Fig. 2. Eventually, we will set μ by demanding

$$\frac{\partial \langle H \rangle}{\partial \mu} = 0, \quad (6)$$

which will tune the average boson occupancy to unity.

The next step towards obtaining a consistent theory is to introduce interplaquette terms. We deduce the form of these terms by considering two coupled hexagons in the following section. Before giving details of our plaquette-operator theory, we illustrate the approach by an analogy to spin-wave theory. Consider a spin- S system that has Neel order at zero temperature. To zeroth order, this is described as a classical system of antialigned spins with each spin of length S . This is analogous to our isolated plaquette limit with $\bar{p} = 1$ which has perfect plaquette ordering. Standard linear spin-wave theory takes into account quantum fluctuations about the Néel state and gives the spectrum of low-lying excitations. Spin waves reduce the length of the ordered moment and give rise to zero-point energy corrections. Analogously, our plaquette-operator theory captures the low-lying excitations about the pRVB state. These corrections will reduce the value of \bar{p} and modify the ground-state energy in a self-consistent manner.

A. Coupling two hexagons

Figure 4 shows two nearest-neighbor hexagons, A and B, and the five bonds which couple them. The five Heisenberg-like bonds act as a perturbation, which we denote as H_{AB} , coupling the single-hexagon states of A and B. In the absence of this perturbation, any eigenstate is a direct product of single-hexagon states centered on A and B, $|A_u B_v\rangle$, signifying that the A hexagon is in the $|u\rangle$ state and B is in the $|v\rangle$ state.

The matrix element of H_{AB} between two direct product states, $|A_u B_v\rangle$ and $|A_p B_q\rangle$, is given by

$$\begin{aligned} & \langle A_u B_v | H_{AB} | A_p B_q \rangle \\ &= \sum_b \sum_{\alpha=x,y,z} J_b \langle A_u B_v | S_{i_b,A,\alpha} S_{j_b,B,\alpha} | A_p B_q \rangle. \end{aligned} \quad (7)$$

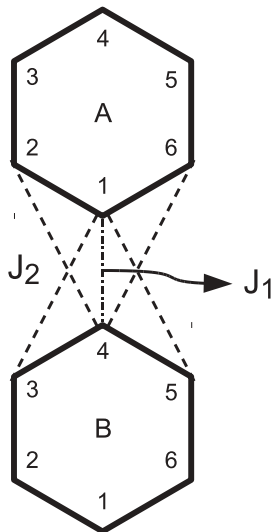


FIG. 4. Coupling between two nearest-neighbor hexagons, A and B. The dotted lines denoted Heisenberg-like exchange terms which couple A and B.

The index b sums over the interhexagon bonds which connect site i_b of hexagon A and site j_b of hexagon B (see Fig. 4). Each bond has an exchange coupling strength J_b (given by J_1 for one bond and J_2 for four other bonds).

This quantity reduces to a product of matrix elements of single-hexagon operators,

$$\langle A_u B_v | H_{AB} | A_p B_q \rangle = \sum_b \sum_{\alpha=x,y,z} J_b \langle A_u | S_{i_b, A, \alpha} | A_p \rangle \times \langle B_v | S_{j_b, B, \alpha} | B_q \rangle. \quad (8)$$

Using Eq. (8), we arrive at the following lemma. Note that our motivation is to study the pRVB state in which each hexagon is predominantly in the “−” state.

Lemma. If hexagon A is initially in a singlet state, the coupling hamiltonian H_{AB} will take it to a triplet state. In particular, if A is initially in the “−” state, then the coupling matrix element in Eq. (8) can be nonzero only if A_u —the final state—is a triplet. This is a consequence of the rotation properties of the spin operator $S_{i_b, A, \alpha}$ which acts as a triplet under rotation.

We make the following assertions using this lemma.

(i) $\langle A_- B_- | H_{AB} | A_- B_- \rangle = 0$. Thus, the strict plaquette RVB state which has both hexagons in the pure “−” state is not preserved under the coupling Hamiltonian. In the bosonic representation, the interplaquette coupling does not lead to terms of the form $b_{A,-}^\dagger b_{B,-}^\dagger b_{A,-} b_{B,-}$ (equivalently, \bar{p}^4). In the condensed state, after taking interplaquette terms into account, there is no term proportional to \bar{p}^4 in the Hamiltonian.

(ii) Similarly, $\langle A_- B_- | H_{AB} | A_- B_u \rangle = 0$. There are no terms proportional to \bar{p}^3 in the Hamiltonian.

(iii) $\langle A_u B_v | H_{AB} | A_- B_- \rangle$ can be nonzero only when u and v are triplet states. Furthermore, from conservation of z component of spin, we should have $m_u + m_v = 0$. These matrix elements lead to $\mathcal{O}(\bar{p}^2)$ terms which involve creation/annihilation of pairs of triplets, i.e., we have terms of the form $\bar{p}^2 \{b_{A,u}^\dagger b_{B,v}^\dagger\}$ and $\bar{p}^2 \{b_{B,v} b_{A,u}\}$.

(iv) $\langle A_- B_v | H_{AB} | A_u B_- \rangle$ can be nonzero only when u and v are triplet states. This gives rise to $\mathcal{O}(\bar{p}^2)$ terms which involve hopping of triplet operators, i.e., $\bar{p}^2 \{b_{B,v}^\dagger b_{A,u}\}$.

(v) We can have nonzero matrix elements of the form $\langle A_- B_u | H_{AB} | A_v B_q \rangle$, leading to $\mathcal{O}(\bar{p}^1)$ terms. However, these processes are highly unlikely and can be ignored. This is justified when the pRVB order is strong and each plaquette is predominantly in the “−” state. While the “−” boson is condensed, all other bosons will be present in very dilute concentrations. Thus, interactions between such bosons are unlikely.

(vi) We also have terms independent of \bar{p} which do not involve the “−” state, but these can again be ignored using the above argument.

The above statements drastically simplify the effective coupling between adjacent plaquettes A and B. Our scheme can be justified in two different ways. In the first approach, we expand the Hamiltonian in powers of \bar{p} . Arguing from (i) through (iv) above, we see that the leading terms are $\mathcal{O}(\bar{p}^2)$. These terms are quadratic in triplet operators and involve hopping-like and pairing-like terms discussed in (iii) and (iv) respectively. We retain these leading terms alone and ignore $\mathcal{O}(\bar{p}), \mathcal{O}(1)$ corrections as discussed in (v) and (vi) above.

A second approach is to start with the assumption of strong pRVB order. Every hexagon is predominantly occupied by the “−” boson. All other bosons are present in very dilute quantities. Thus, beginning with (v) and (vi) above, we neglect unlikely interactions between these dilute bosons. Using (i)–(iii), we find that the most likely processes are $\mathcal{O}(\bar{p}^2)$ terms which are quadratic in triplet operators.

The above arguments apply to any pair of nearest-neighbor plaquettes in the honeycomb lattice of Fig. 2. They lead to an effective hamiltonian for the pRVB state which *only* involves the “−” singlet and all triplet bosons. The quintets, heptets, and other singlets simply drop out of the problem. Interaction corrections arising from $\mathcal{O}(\bar{p})$ terms that we have ignored can populate these states. However, we expect these corrections to be small. In the rest of this paper, we ignore the other bosons as they play no role.

B. Effective Hamiltonian for the pRVB state

We have examined the nature of the coupling between nearest-neighbor plaquettes, and deduced that they lead to hopping-like and pairing-like terms in triplet operators. There are no couplings between further neighbors as the microscopic spin Hamiltonian has only short-range interactions. A cursory inspection of Fig. 2 shows that J_1 and J_2 interactions do not couple further neighbors.

The effective theory of the pRVB state can be written as

$$H = \sum_i \sum_{u=\text{triplets}} (\epsilon_u - \mu) b_{i,u}^\dagger b_{i,u} + N \bar{p}^2 (\epsilon_- - \mu) + N \mu + \bar{p}^2 \sum_{(ij)} \sum_{u,v=\text{triplets}} [(h_{uv}^{ij}) b_{i,u}^\dagger b_{j,v} + (d_{uv}^{ij}) b_{i,u}^\dagger b_{j,v}^\dagger + \text{H.c.}]. \quad (9)$$

The first line includes the intraplaquette terms, the index i summing over all shaded plaquettes in Fig. 2. The chemical

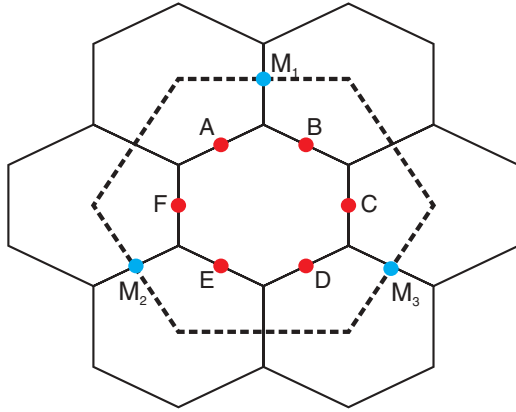


FIG. 5. (Color online) The plaquette Brillouin zone (BZ): The dashed line indicates the BZ of the underlying honeycomb lattice. The pRVB state occurs on a triangular lattice of plaquettes; the corresponding BZ is shown by solid lines using the extended zone scheme. The M points of the plaquette-triangular BZ are highlighted by blue/red circles; these are the wave vectors at which the lowest tripton excitations occur.

potential μ can be tuned to enforce single boson occupancy (on average). N denotes the number of shaded plaquettes in the system.

The second line involves interplaquette terms; the indices u and v sum over *all* 27 triplet states in the single-hexagon spectrum. As argued at the end of the previous section, the quintets, heptets, and singlets other than the “ $-$ ” state drop out of the problem. The coefficients (h_{uv}^{ij}) and (d_{uv}^{ij}) are the amplitudes for triplet hopping and triplet pairing processes. The evaluation of these amplitudes is discussed in the Appendix.

We rewrite the Hamiltonian of Eq. (9) by going to momentum space.²¹ As the plaquettes form a triangular lattice, we obtain a hexagonal Brillouin zone. Figure 5 shows the plaquette Brillouin zone in relation to the hexagonal Brillouin zone of the underlying honeycomb lattice. The Hamiltonian takes the form

$$H = \sum_{\mathbf{k}} \begin{pmatrix} b_{1,\mathbf{k}}^\dagger \\ \vdots \\ b_{27,\mathbf{k}}^\dagger \\ b_{1,-\mathbf{k}} \\ \vdots \\ b_{27,-\mathbf{k}} \end{pmatrix}^T \begin{pmatrix} \hat{H}_{\epsilon,\mu,h}(\mathbf{k}) & \hat{H}_d(\mathbf{k}) \\ \hat{H}_d^\dagger(\mathbf{k}) & \hat{H}_{\epsilon,\mu,h}^T(-\mathbf{k}) \end{pmatrix} \begin{pmatrix} b_{1,\mathbf{k}} \\ \vdots \\ b_{27,\mathbf{k}} \\ b_{1,-\mathbf{k}}^\dagger \\ \vdots \\ b_{27,-\mathbf{k}}^\dagger \end{pmatrix}. \quad (10)$$

The matrix $\hat{H}_{\epsilon,\mu,h}$ involves triplet energies of the single hexagon problem, the chemical potential μ , and hopping terms h_{uv}^{ij} . The off-diagonal blocks \hat{H}_d involve pairing amplitudes d_{uv}^{ij} . The primed sum indicates that if \mathbf{k} is included, $-\mathbf{k}$ is to be excluded.

The eigenvalue spectrum of this Hamiltonian can be obtained by a bosonic Bogoliubov transformation. These give the energies of “triplon” excitations above the pRVB state. The ground-state energy acquires zero-point energy contributions from these triplon modes. The Hamiltonian has two parameters \bar{p} and μ which are determined self-consistently,

by demanding

$$\frac{\partial \langle H \rangle}{\partial \mu} = 0, \quad (11)$$

$$\frac{\partial \langle H \rangle}{\partial \bar{p}} = 0. \quad (12)$$

Equation (11) tunes the average boson density. We treat \bar{p} as a variational parameter; Eq. (12) minimizes the ground state with respect to \bar{p} .

For any value of $J_2 < 0.5$, the Hamiltonian in Eq. (9) can be derived and diagonalized. (For $J_2 > 0.5$, our plaquette operator theory is not justified as the “ $-$ ” state is not the ground state of the single hexagon problem.) Equations (11) and (12) can then be used to obtain the self-consistent solution. In the self-consistent solution, the eigenvalue of the lowest tripton mode gives the spin gap above the pRVB state.

IV. RESULTS

The plaquette-operator mean-field theory is a novel method to study plaquette-ordered phases. Our plaquette-operator calculation is valid in the limit of strong plaquette order, i.e., when \bar{p}^2 is close to unity, as \bar{p}^2 is the probability of finding a plaquette in the “ $-$ ” state. As a consistency check, we plot the self-consistently obtained value of \bar{p}^2 as a function of J_2/J_1 in Fig. 6. We find that pRVB order is strongest around $J_2 \sim 0.25$, where $\bar{p}^2 \sim 96\%$. As seen in the figure, we find $\bar{p}^2 > 90\%$ for $0.15 \lesssim J_2 \lesssim 0.43$. This puts our plaquette-operator approach on a solid basis.

In Fig. 7, we plot the ground state energy obtained from plaquette-operator theory as a function of J_2/J_1 . This is obtained as the zero-temperature expectation value of the Hamiltonian in Eq. (10). To see if the pRVB state is a plausible ground state, we compare its energy with the following estimates:

(i) Néel/spiral state from large- S spin-wave theory: In the semiclassical large- S limit, the ground state has Néel order for $J_2 < J_1/6$ and spiral order for $J_2 > J_1/6$. Linear spin-wave theory gives the energy of low-lying excitations.²² Figure 7 plots the energy of the large- S ground state including zero-

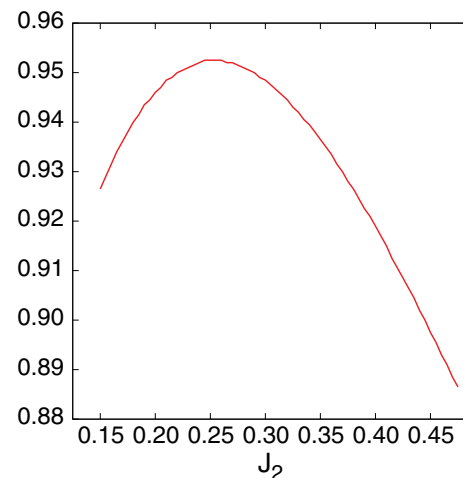


FIG. 6. (Color online) The probability of finding a shaded plaquette in the “ $-$ ” state. \bar{p}^2 as a function of J_2/J_1 . pRVB order is strongest around $J_2 \sim 0.25$.

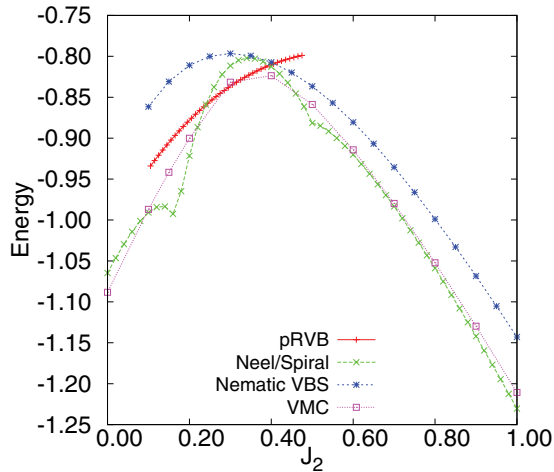


FIG. 7. (Color online) The energy of the pRVB state obtained from plaquette-operator theory. We compare energy per unit cell with other candidate states (see text).

point contributions from spin-wave excitations. To obtain the energy for the spin-1/2 case, we set $S = 1/2$ in the spin-wave calculation. For $0.22 \lesssim J_2 \lesssim 0.4$, the pRVB state is lower in energy than the large- S estimate.

(ii) “Nematic valence bond solid”: A dimer state which breaks lattice rotational symmetry has been proposed as the ground state for $J_2 \gtrsim 0.4$.^{23,22} This state can also be viewed as the staggered dimer state on the honeycomb lattice. We plot the energy of this state obtained using bond operator mean-field theory keeping only quadratic terms in triplet operators.²² For $J_2 \lesssim 0.4$, the pRVB state is lower energy than this dimer state.

(iii) Variational Monte Carlo (VMC): Recently, a VMC scheme using entangled-plaquette wave functions has estimated the ground-state energy for the J_1 - J_2 model.¹⁴ Around $J_2 \sim 0.3$, our energy estimate for the pRVB state compares well with the variational result. In fact, the pRVB energy is lower than the VMC result at $J_2 = 0.3$; this may be an artifact of our mean-field theory. Corrections such as triplet-triplet interactions, coupling to quintet states, etc., may of course change the energy of the pRVB state. While the VMC study does not find pRVB order, energy comparison indicates that pRVB is a plausible ground state.

Comparing the energy of the pRVB state with the above candidates, we conclude that the ground state may have pRVB order for $0.25 \lesssim J_2 \lesssim 0.4$. Next, we plot the spin gap as a function of J_2/J_1 ; this is the energy of the lowest triplon state. We find that this lowest triplon state always occurs at the M points of the plaquette Brillouin zone (see Fig. 5). The spin gap reaches a maximum value of $\sim 0.7J_1$ at $J_2 \sim 0.225$. Surprisingly, the spin gap does not close as J_2 is varied. We discuss its implications in the next section.

V. DISCUSSION

We have developed an effective theory for the proposed pRVB state in the spin-1/2 J_1 - J_2 model on the honeycomb lattice. Using plaquette-operator mean-field theory, we have calculated the properties of this state and the spectrum of low-lying excitations above it.

An important outcome of our calculation is to clarify the nature of the pRVB state. The low-energy state is composed of a $\sqrt{3} \times \sqrt{3}$ ordering of plaquettes in the “-” state. We begin our calculation from the limit of decoupled hexagons, wherein the “-” state is clearly lower in energy for $J_2 < 0.5$. After including interhexagon coupling, we get a consistent theory of the pRVB state. Thus, our plaquette wave function changes sign upon rotation by 60° . Under rotation by angle ϕ , the plaquette wave function transforms as $e^{i3\phi}$, having f -wave symmetry.

As we argue below, we have ruled out s -wave pRVB order involving condensation of the “+” state. In the limit of disconnected hexagons, the “+” state is an excited state. As such, we expect s -wave pRVB order to be unstable for this reason. However, strong interhexagon coupling could possibly stabilize this phase by means of a large kinetic gain from delocalizing the triplet excitations. To rule out this possibility, we redid the plaquette operator calculation for the s -wave case. We do not find a consistent s -wave pRVB solution, thus ruling out strong s -wave ordering.

The earliest study of plaquette order on the honeycomb lattice describes s -wave plaquette order in a quantum dimer model. The plaquette wave function is *symmetric* under rotation.²⁴ However, for the J_1 - J_2 model at hand, Ref. 12 indicates that the antisymmetric combination is favored; the authors refer to this order as d -wave, while it is more precisely called f -wave. We reaffirm this f -wave nature using our plaquette operator approach.

A. Excitations of pRVB state

This paper presents a systematic study of the pRVB state and its excitations. As shown in Fig. 8, the spin gap does not close within our theory. Also, the lowest-lying triplet modes occur at the M points of the plaquette BZ. In terms of the underlying honeycomb lattice, the lowest triplet state will occur at wave vectors shown in Fig. 5. Assuming that pRVB

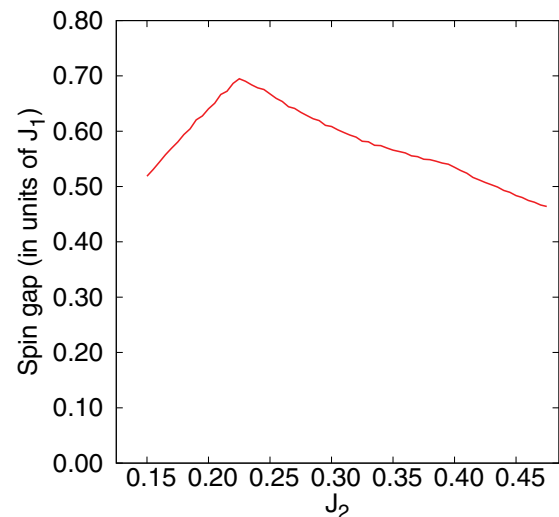


FIG. 8. (Color online) The spin gap obtained from plaquette-operator theory as a function of J_2 . The gap is in units where J_1 is unity.

order occurs in the J_1 - J_2 model, numerical methods such as exact diagonalization or DMRG can see this by calculating the spin-spin structure factor in the lowest triplet state. The structure factor should show peaks at the wave vectors shown in Fig. 5. Indeed, this can serve as a test for pRVB order.

As is familiar from the study of dimer states,²⁵ an applied magnetic field will lower the energy of triplet modes. At some critical field, the lowest triplet mode(s) will become gapless and undergo Bose condensation giving rise to magnetic order. In our case, the lowest triplet modes are triply degenerate as they occur at the three M points of the plaquette BZ. Beyond the critical field, each mode can condense with an independent amplitude and phase leading to six degrees of freedom. This makes it difficult to predict the nature of the magnetic ordering beyond the critical field. At the level of these arguments, we can rule out field-induced Néel ordering as the lowest triplets do not occur at the Γ point. This picture may change once we account for defects in pRVB order as discussed below.

B. Phase transitions

For the case of dimer-Néel transitions, bond operator theory is remarkably successful in describing the nature of the phase transition. Starting from the dimer state, bond operator theory provides a consistent theory of spin-1 triplon excitations which obey bosonic statistics. The transition to Néel order occurs via Bose condensation of triplons when the spin gap closes.^{16,26}

In our honeycomb lattice model, our plaquette operator theory gives a consistent description of the pRVB state which is most stable around $J_2 \sim 0.25$. ED calculations suggest that a pRVB state is sandwiched between a Néel state (for $J_2 \lesssim 0.2$) and a magnetic phase with stripe order (for $J_2 \gtrsim 0.4$). While the phase diagram definitely contains Néel order, the existence of a stripe magnetic phase is still open to question. It has been suggested that the ground state for $J_2 \gtrsim 0.4$ has dimer order which breaks lattice rotational symmetry.^{22,23}

Starting from the pRVB state, as J_2 is decreased, we expect to see a Néel transition near $J_2 \sim 0.2$. Naïvely, we may expect such a transition to be driven by condensation of triplons giving rise to a continuous quantum phase transition (QPT) in the same universality class as the BEC transition in $2+1$ dimensions. However, the spin gap obtained from plaquette operator theory does not close as J_2 is lowered, thus ruling out a BEC transition. This leaves us with two possibilities concerning the pRVB-Néel transition: (i) a first-order phase transition, or (ii) a deconfined QPT mediated by topological defects in pRVB order. In terms of conventional Landau theory, we generically expect a first-order QPT as the Néel state and pRVB state break different symmetries. This is always a possibility and can only be checked using precise numerical techniques. The second possibility, a deconfined QPT,^{27,28} is a very exciting prospect. So far, such a transition has not been observed in simple models involving Heisenberg-like couplings.

A deconfined QPT would be driven by proliferation of defects in the pRVB order parameter; in this case, Z_3 vortices. As pointed out in Ref. 29, the core of such a vortex will necessarily bind a dangling spin or a “spinon”. The critical theory of a continuous pRVB-Néel transition cannot be cast in terms of Landau-Ginzburg order parameters, but in terms

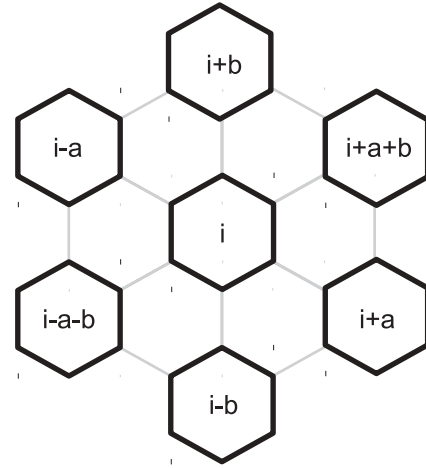


FIG. 9. A plaquette i and its nearest neighbors. \hat{a} and \hat{b} are the primitive vectors of the $\sqrt{3} \times \sqrt{3}$ lattice of plaquettes.

of these spinful defects. We expect the theory to be very similar to the one outlined in Ref. 28; at the critical point, the vortices become gapless and the Z_3 anisotropy may become irrelevant.

Starting from the pRVB state, when we increase J_2 , there must be a transition into a state which breaks lattice rotational symmetry; a nematic valence bond solid²² or a magnetic phase with stripe order.¹² The spin gap does not close in our plaquette operator theory. As suggested by ED results,¹² we surmise that this is a first-order transition. Future numerical studies will be able to test this notion.

ACKNOWLEDGMENTS

We thank I. Rousochatzakis for many helpful discussions.

APPENDIX: MATRIX ELEMENTS

Figure 9 shows a plaquette i and its six nearest neighbors. Let us first consider the nearest-neighbor pair $(i, i - \hat{b})$. This pair is identical to that shown in Fig. 4 if we identify (i) as A and $(i - \hat{b})$ as B. Interplaquette coupling leads to hopping-like and pairing-like terms between triplon operators on the two sites. Below, we evaluate the coefficients $h_{uv}^{i, i - \hat{b}}$ and $d_{uv}^{i, i - \hat{b}}$.

The generic inter-plaquette interaction process is indicated in Eq. (8). The hopping-like term arises the following matrix element:

$$h_{uv}^{i, i - \hat{b}} = \langle (i)_u (i - \hat{b})_v | H_{i, i - \hat{b}} | (i)_u (i - \hat{b})_v \rangle. \quad (A1)$$

This matrix element can be evaluated numerically using two pieces of information: (i) the explicit eigenstates of the single hexagon problem and (ii) the explicit form of the interplaquette coupling given in Eq. (8). In plaquette operator notation, this matrix element leads to the process $b_{i,u}^\dagger b_{i-\hat{b},-}^\dagger b_{i,-} b_{i-\hat{b},v}$. As the “-” bosons are condensed with amplitude \bar{p} , we rewrite this as

$$H_{\text{hopping}} \sim h_{uv}^{i, i - \hat{b}} \bar{p}^2 b_{i,u}^\dagger b_{i-\hat{b},v}. \quad (A2)$$

Similarly, the coefficient of the pairing term is given by

$$d_{uv}^{i,i-\hat{b}} = \langle (i)_u (i-\hat{b})_v | H_{i,i-\hat{b}} | (i)_-(i-\hat{b})_- \rangle. \quad (\text{A3})$$

This gives rise to $b_{i,u}^\dagger b_{i-\hat{b},v}^\dagger b_{i,-} b_{i-\hat{b},-}$, which can be rewritten as

$$H_{\text{pairing}} \sim d_{uv}^{i,i-\hat{b}} \bar{p}^2 b_{i,u}^\dagger b_{i-\hat{b},v}^\dagger. \quad (\text{A4})$$

Having evaluated these terms for one nearest-neighbor pair, we can evaluate the matrix elements for all other pairs using the rotation operator. Let us consider three nearest-neighbor pairs in Fig. 9: $(i, i-\hat{b})$, $(i, i+\hat{a})$, and $(i, i+\hat{a}+\hat{b})$. Clearly, these three pairs are related by \hat{R} , rotation by 60° , about the center of the hexagon i . Formally, in terms of the inter-plaquette couplings, we may write

$$H_{i,i+\hat{a}} = \hat{R} H_{i,i-\hat{b}} \hat{R}^\dagger. \quad (\text{A5})$$

The rotation operator \hat{R} maps the plaquette $(i-\hat{b})$ to $(i+\hat{a})$. In addition, it rotates the hexagons by 60° .

Using this relation, we can obtain the hopping matrix element $h_{uv}^{i,i+\hat{a}}$:

$$\begin{aligned} h_{uv}^{i,i+\hat{a}} &= \langle (i)_u (i+\hat{a})_v | H_{i,i+\hat{a}} | (i)_-(i+\hat{a})_- \rangle \\ &= \langle (i)_u (i+\hat{a})_v | \hat{R} H_{i,i-\hat{b}} \hat{R}^\dagger | (i)_-(i+\hat{a})_- \rangle \\ &= r_u r_v^* \langle (i)_u (i-\hat{b})_v | H_{i,i-\hat{b}} | (i)_-(i-\hat{b})_- \rangle \\ &= r_u r_v^* h_{uv}^{i,i-\hat{b}}, \end{aligned} \quad (\text{A6})$$

where r_u and r_v are the rotation eigenvalues of the single-hexagon states $|u\rangle$ and $|v\rangle$ respectively.

The coefficient of the pairing-like term can be found likewise:

$$\begin{aligned} d_{uv}^{i,i+\hat{a}} &= \langle (i)_u (i+\hat{a})_v | H_{i,i+\hat{a}} | (i)_-(i+\hat{a})_- \rangle \\ &= \langle (i)_u (i+\hat{a})_v | \hat{R} H_{i,i-\hat{b}} \hat{R}^\dagger | (i)_-(i+\hat{a})_- \rangle \\ &= r_u r_v (r_-^*)^2 \langle (i)_u (i-\hat{b})_v | H_{i,i-\hat{b}} | (i)_-(i-\hat{b})_- \rangle \\ &= r_u r_v (r_-^*)^2 d_{uv}^{i,i-\hat{b}}. \end{aligned} \quad (\text{A7})$$

Similarly, by applying one more rotation, we can obtain

$$h_{uv}^{i,i+\hat{a}+\hat{b}} = r_u^2 (r_v^*)^2 h_{uv}^{i,i-\hat{b}}, \quad d_{uv}^{i,i+\hat{a}+\hat{b}} = r_u^2 r_v^2 (r_-^*)^4 d_{uv}^{i,i-\hat{b}}.$$

*g.ramachandran@ifw-dresden.de

¹D. Sen, B. S. Shastry, R. E. Walstedt, and R. Cava, *Phys. Rev. B* **53**, 6401 (1996); T. Nakamura and K. Kubo, *ibid.* **53**, 6393 (1996).

²O. A. Starykh, R. R. P. Singh, and G. C. Levine, *Phys. Rev. Lett.* **88**, 167203 (2002).

³Z. Y. Meng, T. C. Lang, S. Wessel, F. F. Assaad, and A. Muramatsu, *Nature (London)* **464**, 847 (2010).

⁴O. Smirnova, M. Azuma, N. Kumada, Y. Kusano, M. Matsuda, Y. Shimakawa, T. Takei, Y. Yonesaki, and N. Kinomura, *J. Am. Chem. Soc.* **131**, 8313 (2009).

⁵R. Ganesh, D. N. Sheng, Y.-J. Kim, and A. Paramekanti, *Phys. Rev. B* **83**, 144414 (2011).

⁶S. Okumura, H. Kawamura, T. Okubo, and Y. Motome, *J. Phys. Soc. Jpn.* **79**, 114705 (2010).

⁷F. Wang, *Phys. Rev. B* **82**, 024419 (2010).

⁸Y.-M. Lu and Y. Ran, *Phys. Rev. B* **84**, 024420 (2011).

⁹B. K. Clark, D. A. Abanin, and S. L. Sondhi, *Phys. Rev. Lett.* **107**, 087204 (2011).

¹⁰P. H. Y. Li, R. F. Bishop, D. J. J. Farnell, and C. E. Campbell, *Phys. Rev. B* **86**, 144404 (2012).

¹¹H. Mosadeq, F. Shabazi, and S. A. Jafary, *J. Phys.: Condens. Matter* **23**, 226006 (2011).

¹²A. F. Albuquerque, D. Schwandt, B. Hetényi, S. Capponi, M. Mambrini, and A. M. Läuchli, *Phys. Rev. B* **84**, 024406 (2011).

¹³J. Reuther, D. A. Abanin, and R. Thomale, *Phys. Rev. B* **84**, 014417 (2011).

¹⁴F. Mezzacapo and M. Boninsegni, *Phys. Rev. B* **85**, 060402 (2012).

¹⁵D. J. J. Farnell, R. F. Bishop, P. H. Y. Li, J. Richter, and C. E. Campbell, *Phys. Rev. B* **84**, 012403 (2011).

¹⁶S. Sachdev and R. N. Bhatt, *Phys. Rev. B* **41**, 9323 (1990).

¹⁷Y. Matsushita, M. P. Gelfand, and C. Ishii, *J. Phys. Soc. Jpn.* **68**, 247 (1999).

¹⁸A. W. Sandvik and D. J. Scalapino, *Phys. Rev. Lett.* **72**, 2777 (1994).

¹⁹B. Kumar, *Phys. Rev. B* **82**, 054404 (2010).

²⁰L. Isaev, G. Ortiz, and J. Dukelsky, *Phys. Rev. B* **79**, 024409 (2009).

²¹We use the transform convention $b_{i,u} \equiv \frac{1}{\sqrt{N}} \sum_{\mathbf{k}} b_{\mathbf{k},u} e^{i\mathbf{k}\cdot\mathbf{r}_i}$. The wave vectors \mathbf{k} lie in the plaquette Brillouin zone shown in Fig. 5.

²²A. Mulder, R. Ganesh, L. Capriotti, and A. Paramekanti, *Phys. Rev. B* **81**, 214419 (2010).

²³J. B. Fouet, P. Sindzingre, and C. Lhuillier, *Eur. Phys. J. B* **20**, 241 (2001).

²⁴R. Moessner, S. L. Sondhi, and P. Chandra, *Phys. Rev. B* **64**, 144416 (2001).

²⁵T. Nikuni, M. Oshikawa, A. Oosawa, and H. Tanaka, *Phys. Rev. Lett.* **84**, 5868 (2000).

²⁶Ch. Rüegg, A. Furrer, D. Sheptyakov, Th. Strässle, K. W. Krämer, H.-U. GÜdel, and L. Mélési, *Phys. Rev. Lett.* **93**, 257201 (2004).

²⁷T. Senthil, A. Vishwanath, L. Balents, S. Sachdev, and M. P. A. Fisher, *Science* **303**, 1490 (2004).

²⁸M. Levin and T. Senthil, *Phys. Rev. B* **70**, 220403 (2004).

²⁹C. Xu and L. Balents, *Phys. Rev. B* **84**, 014402 (2011).